EC Contract No. FP7 - 284877

Virtual certification of acoustic performance for freight and passenger trains

D2.1: User guide describing procedures for modelling wheels and tracks

Due date of deliverable: 30/06/2012

Actual submission date: 21/06/2012

Leader of this Deliverable: Benjamin BETGEN, Nicolas VINCENT, VIBRATEC (VTC)

Reviewed: Y

Document status		
Revision	Date	Description
1	12/06/2012	First issue
2	12/06/2012	Revision including comments from quality review
3	21/06/2012	Approved by TMT
4	21/06/2012	Final version

Project co-funded by the European Commission within the Seven Framework Programme (2007-2013)		
Dissemination Level		
PU	Public	X
PP	Restricted to other programme participants (including the Commission Services)	
RE	Restricted to a group specified by the consortium (including the Commission Services)	
CO	Confidential, only for members of the consortium (including the Commission Services)	

Start date of project: 01/10/2011 Duration: 36 months

Collaborative project

EXECUTIVE SUMMARY

The present document gives guidelines of how to model wheels and tracks for the prediction of rolling noise. As TWINS is widely used for such calculations, recommendations for parameter settings mainly refer to TWINS. However, the aim is to define reasonable modelling hypotheses, independently of the used model.

A set of benchmark calculations has been performed by ISVR, TNO, D2S and VTC. The benchmark cases have been defined in respect to all important parameters that are usually known. The analysis of results has helped to determine sensitive parameters for which different users often define different “default values”. Some of the benchmark results are presented as examples.

TABLE OF CONTENTS

1. INTRODUCTION

Due to the large number of parameters and sub-models available in a model such as TWINS (Track Wheel Interaction Noise Software), significant differences can be obtained by different users. This report defines common calculation procedures to ensure that two different users will obtain similar results for a given wheel/track combination. For more details concerning TWINS, the reader is referred to the existing theoretical manual (1) and user's guide (2). The primary aim of this report is not to reproduce this information, but to define modelling procedures that are also transposable to different models. However, TWINS contains a certain number of parameters for which no recommendations are given in the existing TWINS user's guide. These are discussed in the present document in order to harmonize the "default values" that are used today by the different users.

General recommendations for rolling noise calculations are given in section 2. Sections 3 and 4 contain recommendations for wheel and track modelling respectively.

The present report also includes a presentation and discussion of some of the benchmark calculations that have been performed by ISVR, TNO, D2S and VTC. These are dealt with in section 5.

2. GENERAL RECOMMENDATIONS

General parameters include quantities such as wheel load and train speed. As these of course depend on the rolling stock to be considered, no general recommendations can be given. However, it is important to note that comparability is only assured for a common set of parameters. A possible scenario would for example be to change the wheels of an existing rolling stock and at the same time to decrease the wheel load. Both modifications will have an effect on rolling noise. An advantage of the computational approach is that both effects can be assessed separately.

Effect of speed

The train speed determines the conversion of the roughness wavelength to frequency. An increase of speed corresponds to a translation of the roughness spectrum to higher frequencies. As the roughness amplitude is generally decreasing with frequency (i.e. with decreasing wavelength), this leads to increasing excitation at constant frequency (the TSI+ roughness slope is of 6 dB/ octave, leading to a 6 dB increase for doubling speed).

Additionally, the contact filter always leads to an attenuation of small roughness wavelength excitation ("spatial averaging" of the roughness within the contact area). Above a certain cut-off frequency, the attenuation is of approximately 9 dB/ octave. Identically to the roughness spectrum, an increase of speed corresponds to a translation of the filter curve towards higher frequencies and thus to an increase of the excitation level of 9 dB for doubling speed (for a given frequency above the cut-off frequency). As the wheel contribution is important at relatively high frequencies, the 9 dB/octave slope is often assumed for wheel noise. The proposed (simplified Remington) contact filter function is given in section 2.3.

The influence of changing wheel receptances (due to rotational effects) is much lower than the effect of changing excitation. Therefore, the effect of speed is often accounted for by changing the total filtered roughness only. Although this approach is valid for most cases, it is preferable to introduce the effect of speed throughout the whole calculation process.

Effect of static load

Similarly, the static wheel load has an effect on the contact filter. An increase of load leads to an increase of the contact patch diameter and therefore to an attenuation of high frequency excitation of the wheel. However, the relationship is non linear (doubling the load from 50 kN to 100 kN leads to an increase of the contact patch diameter of roughly 25 % for a standard wheel). The effect of static wheel load on the contact filter is therefore much lower than for the speed. At the same time, its effect on the rail wheel interaction is higher than this is the case for speed. Especially the rail radiated power at high frequencies can be increased by an increase of static load. This is due to a decrease of the contact receptance which results in a higher excitation of the rail (except at the natural frequencies of the wheel, where all relative displacement is absorbed by the wheel). For these reasons, the correct wheel load should be used throughout the whole calculation process.

2.1 TRACK AND ROLLING STOCK INDEPENDENT SETTINGS

Frequency settings

Results should be given in third octave bands from 100 Hz to 5 kHz, i.e. calculations should be carried out in the range from 80 Hz to 6 kHz. The frequency resolution must be high enough to reproduce the dynamics of wheel and track. A variable frequency step can be used to accelerate computations. The maximum frequency step should not exceed 50 Hz and the level difference between two neighbouring frequencies should be below 3 dB.

Number of contact points

In order to take into account the lateral travelling of the wheel on the rail, three contact points should be used for calculations. According to European Standard EN 13979-1 (3) these are chosen at 60 mm, 70 mm and 80 mm from the wheel flange back. The wheel power is determined for each contact point and averaged according to

$$L_W = 10\log_{10}\left(\left(10^{L_W(60mm)/10} + 10^{L_W(70mm)/10} + 10^{L_W(80mm)/10}\right)/3\right) \qquad \textbf{2-1}$$

When using TWINS, it is not necessary to create one separate wheel modal data file for each contact point; a lateral offset of +/- 10 mm from the 70 mm contact point can be defined during TWINS calculations and is taken into account in the wheel dynamics.

For wheels with a coned profile, the contact point on the rail remains fixed, even when the wheel is travelling laterally. Concerning the track, identical results are therefore found for these three wheel contact points. The contact position on the rail is dealt with in section 4.2.

Sound pressure level calculation settings

The sound pressure level is most often requested at 7.5 m. Note that in TWINS, the distance to the (nearest) rail has to be specified (which leads to 6.75 m) and the vertical direction is defined downwards (so that the receiver height has to be set to – 1.2 m).

Ground absorption can be accounted for in various ways, for example by using a reflection coefficient or a flow resistivity of the ground. A (constant) flow resistivity leads to a frequency dependent ground impedance (Delany-Bazley model), which is more realistic than a constant reflection coefficient. This option is therefore preferred. Also, the phase relation between direct and reflected waves (leading to the “ground dip”) is only taken into account in TWINS when using the flow resistivity.

Other settings in fact depend on the rolling stock, such as the number of wheel sets per car and the car length. In accordance with TSI, the SPL should be averaged over a car length. The “accumulation length”, however, can be set to infinity (i.e. to 0 in TWINS). This means that the rail vibration induced by other wheels is taken into account. In reality, the rail vibration coming from a given wheel may rather be reflected by the neighbouring wheel; As these reflections are not taken into account by TWINS, the resulting energy loss is compensated for by including the rail vibration coming from “far away wheels”.

2.2 WHEEL AND RAIL ROUGHNESS

It is well known that wheel and rail roughness have an important effect on rolling noise. This is true for the absolute noise level, but also concerning the spectral content. Therefore the considered roughness spectra can be determining for the relative contribution of rail and wheel. Unfortunately, rail as well as wheel roughness change over time and their measurement is quite costly. The advantage of the computational approach is that the influence of changing roughness is fully eliminated. Two configurations can be compared using exactly the same roughness spectra.

For rail roughness, a limit curve is defined in the TSI noise (see appendix A.3) that can be used for computations. For wheel roughness, no such limit curves exist. Different measured roughness spectra are used from case to case. For cases where only a comparison between two wheel designs is needed, the TSI limit curve for rail roughness can be used as a combined wheel-rail roughness. This in fact eliminates another variable that is complicating the comparability between different computations.

N.B.: Alternatively, transfer functions between a unitary roughness (roughness of 1 m in each frequency band) and radiated power or SPL at 7.5 m can be used in order to eliminate the effect of roughness.

2.3 CONTACT FILTER

The most currently used contact filter is given by

$$|H(f)|^2 = \left[1 + 2\pi^4 \left(\frac{fa}{v}\right)^3\right]^{-1}, \qquad \textbf{2-2}$$

with f the frequency, a the semi-axis length of the contact patch in rolling direction and v the train speed. This filter is often referred to as the “Remington filter”, although equation 2-2 actually represents an approximation of the filter proposed by Remington (4) by a simple filter function.

The contact patch dimension (given by a) depends on the load and the wheel and railhead diameters, typical values for a are around 6 mm.

Figure 2-1 shows an example of such a filter, for a = 5.69 mm and v = 100 km/h. For comparison, a filter corresponding to the “distributed point reacting spring” (DPRS) model [see references (5) and (6) for details] is also plotted. The numerical values plotted here are taken from (7). At low frequencies, the DPRS filter is believed to be less reliable; the formulation according to equation 2-2 is therefore recommended for low frequencies. For simplicity, we recommend the use of the simplified filter given by equation 2-2 for the entire bandwidth if the considered speed is at least 80 km/h.

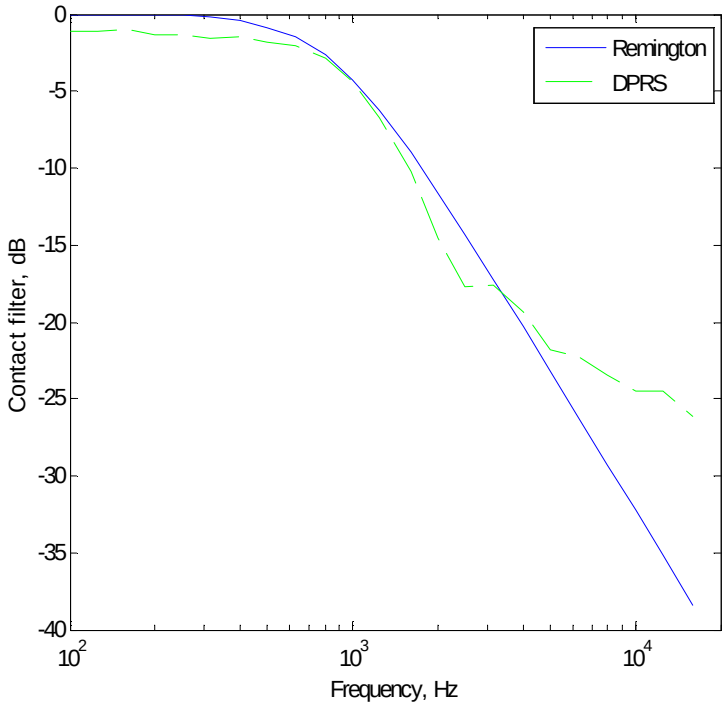

Figure 2-1 : Contact filtering effect for a=5.69 mm and v=100 km/h

N.B.: At small wavelengths (high frequencies), the DPRS filter leads to lower attenuation than the "Remington filter". This may be due to the fact that the DPRS model takes into account the distribution of normal load across the contact zone (7).

For the current settings (at 100 km/h), the difference between both filters is negligible until 5 kHz; the effect on overall SPL is therefore very low. For speeds above 100 km/h, both filters lead to essentially identical results over the entire considered bandwidth (100 Hz – 6 kHz).

The speed of 80 km/h which is important for the homologation of freight rolling stock can be seen as a limit case. Indeed, the difference between both filters becomes visible at this speed. At present, it is not entirely proven that the DPRS filter is the more realistic filter model, however. More experimental evidence is needed. The simplified filter model according to equation 2-2 is therefore recommended for speeds ≥ 80 km/h. For any calculation case, the choice of the filter model has to be documented.

3. WHEEL MODELLING

As far as rolling noise calculations are concerned, railway wheels may be classified according to the following categories:

1. Axis-symmetrical monobloc wheels
2. Non axis-symmetrical monobloc wheels
3. Wheels with flanged brake discs (to be considered as non axis-symmetrical)
4. Resilient wheels
5. Wheels with dampers

The majority of railway wheels for mainline applications are axis-symmetrical monobloc wheels. These are dealt with in the present report, excluding for example resilient wheels or wheels with flanged brake discs. Some of the categories 2 to 5 are addressed in ACOUTRAIN Task 2.6, however.

Finite Element (FE) models of (bare) axis-symmetrical monobloc wheels are reliable. The discrepancy between calculated and measured natural frequencies does generally not exceed a few percent. As damping can generally not be calculated, the need for measurements is rather related to the question of how to determine the wheel modal damping. For axis-symmetrical monobloc wheels, the measurement of damping is in fact not necessary (see also paragraph 3.3).

3.1 MESHING

Nowadays, the use of axis-symmetrical models is not compulsory anymore for reasons of computational cost. Note, however, that the TWINS model is based on the hypothesis of an axis-symmetrical wheel, and the wheel modal basis has to be provided in a particular format (.mp file). The creation of this file seems easier when using an axis-symmetrical wheel model, especially in regard of the modal damping which depends on the number of nodal diameters n (see also section 3.3). The usage of 3D brick elements (only translational degrees of freedom) can also lead to satisfying results though.

Element dimensions of about 5mm in regions with high deformations (axis-symmetrical model) have been shown to be sufficient. Indeed, the mesh displayed in Figure 3-1 could be sparser near the hub; however, the computational time for the resolution of such axis-symmetrical models is very short. Quadratic elements (in ANSYS type 183 elements) are preferred because of a higher precision at the same element size. However, when using a 5 mm mesh size, the results obtained with linear and quadratic elements differ little. (see also appendix B.1).

One node on the running surface should be placed exactly at 70 mm from the wheel flange (nominal contact point). TWINS allows defining an offset from the nominal contact point for excitation of the wheel at 60 mm and 80 mm.

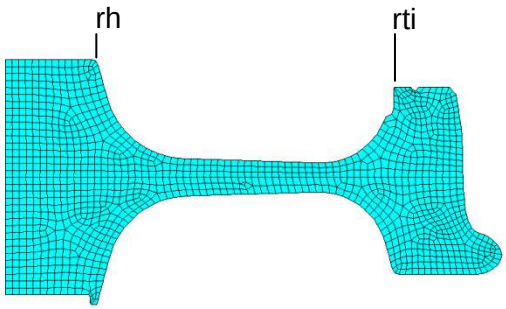

Figure 3-1 : Wheel mesh example (VB2N wheel), indication of hub radius (rh) and inner tyre radius (rti), meshing performed by ISVR

3.2 RESPONSE POSITIONS

The wheel tread itself hardly deforms in the considered frequency range; it is rather subject to radial and rocking motion as a whole. TWINS uses the nominal contact point at 70 mm to assess radial motion and a point on the outer side of the tread (half way between the inner tyre radius rti and the radius of the running plane) for axial motion. Radiation of the web in contrast has to be estimated from the lateral displacement of the web at a higher number of nodes. In TWINS, these nodes are chosen by the user when constructing the wheel modal input data file from the FE results. It is recommended to distribute these points regularly between hub radius and inner tyre radius of the wheel (rh and rti in Figure 3-1). We propose a distribution according to the following rule:

r1=rh+(rti-rh) /10

r2= rh+3*(rti-rh) /10

r3= rh+5*(rti-rh) /10

r4= rh+7*(rti-rh) /10

r5= rh+9*(rti-rh) /10

rh being the hub radius and rti the inner tyre radius.

As mentioned above, a 6^{th} node on the outer side of the wheel tread is chosen half way between the inner tyre radius rti and the radius of the running plane.

A small deviation from this rule will have no effect on the calculated results. Therefore, the definition of anchor nodes at these exact positions prior to meshing is not necessary. Also, a comparison between calculations with wheel modal data files using 4 or 5 web positions shows negligible differences of unitary powers : The maximum difference in wheel power remains below 0.3 dB for $1/3^{rd}$ octave bands between 500 Hz and 5 kHz. In certain lower frequency bands the differences have been found to be slightly higher (maximum difference of 1.5 dB at 200 Hz), however, the difference of overall filtered wheel power was below 0.01 dB(A).

3.3 WHEEL MODAL DAMPING

It is important to note that under rolling conditions the railway wheel is subject to internal losses (modal damping) as well as to a loss of energy due to the contact with the rail (so called “damping when rolling”). Whenever the “damping when rolling” is higher than the wheel modal damping, an exact measurement of the latter is not necessary. This is the case for (bare) monobloc wheels that have very low modal damping ratios. Additionally, modal damping differs little from one (axis-symmetrical monobloc) wheel design to another. It essentially depends on the damping introduced by the axle through coupling between axle modes and wheel modes. This coupling in turn depends on the number of nodal diameters of the considered wheel mode.

Typically, the following values are used (given in $c/c_c = ½\ \eta$, as requested for the TWINS wheel modal parameters file) :

- $\zeta_i = c/c_c = 0.001$ for $n_i = 0$ (medium damping due to coupling with extension of the axle)
- $\zeta_i = c/c_c = 0.01$ for $n_i = 1$ (high damping due to coupling with bending of the axle)
- $\zeta_i = c/c_c = 0.0001$ for $n_i \geq 2$ (low coupling)

Experimentally, the radial mode R1 can generally not be found at all. Indeed, its damping due to coupling with the axle is even higher than for axial modes of order n = 1. A damping ratio between $\zeta = 0.2$ and $\zeta = 1$ is generally applied in order not to overestimate the contribution of this mode[1].

For the reasons given above, the purely computational approach has widely been accepted as reliable for axis-symmetrical monobloc wheels (cf. EN 13979-1 (3)).

Whenever the wheel modal damping ratios in free-free conditions approach the damping introduced through the wheel-rail contact, these have to be determined experimentally. This is the case for wheels with dampers and resilient wheels, but also for wheels with flanged brake discs (friction between discs and wheel). These aspects are not detailed in this report, however.

[1] The difference between these values is expected to be very small. Indeed, when using a damping ratio of $\zeta = 0.2$, mode R1 is hardly detectable anymore on the calculated wheel receptance.

4. TRACK MODELLING

In contrast to the wheel, the track can be modelled fully analytically if certain simplifications are introduced. On the other hand, various parameters and modelling assumptions have an influence on calculation results. For this reason, coherent results between different users are more difficult to obtain when the track is concerned.

Figure 4-1 (taken from the benchmark calculations) shows that the rail radiated power can be very different from one track to another, which is hardly surprising. If a particular track shall be reproduced by calculations, a good knowledge of its characteristics is therefore important.

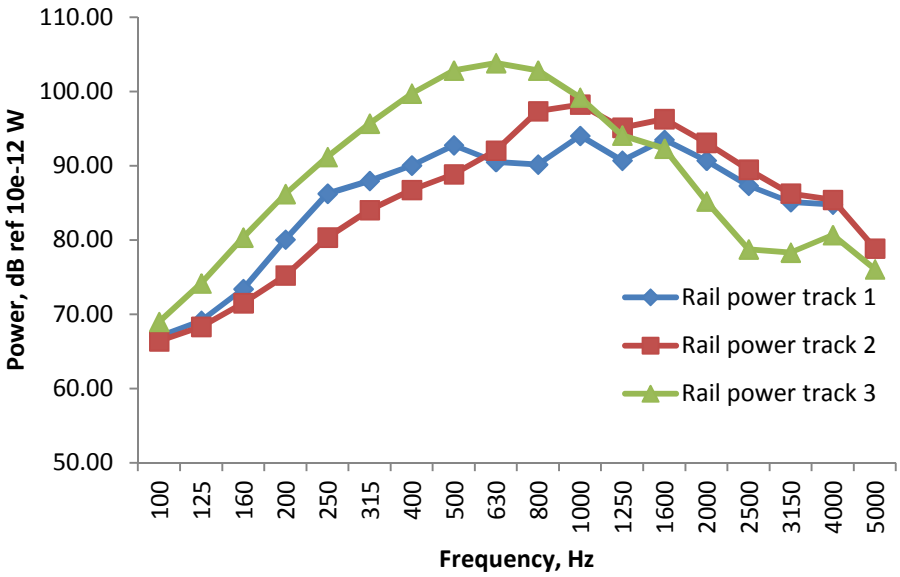

Figure 4-1 : Rail radiated power for different tracks, calculated decay rates (ISVR calculations at 160 km/h using TSI roughness as total roughness), see section 4.1 for details on the various tracks.

As Figure 4-2 suggests, wheel power is in contrast fairly independent of the used track, at least in the higher frequency range where the wheel contribution is important (note that the presented figures are *not* A-weighted). For virtual homologation of rolling stock, the track modelling may therefore have less importance. On the other hand, the total power of course includes the effect of the track. The same change in wheel power can therefore lead to a significant change in total power or not – depending on the track contribution.

Besides a guideline of how to model tracks, the definition of reference tracks is therefore important.

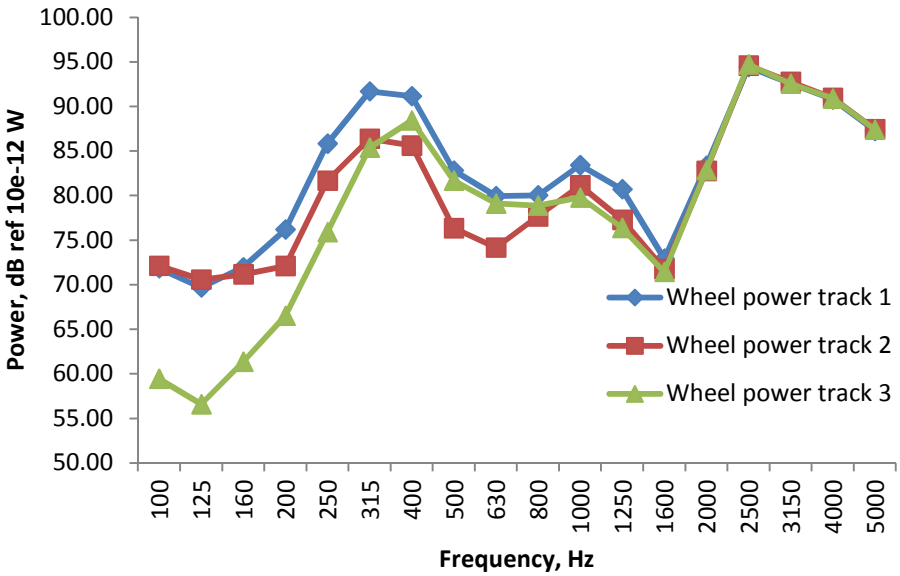

Figure 4-2 : Wheel (VB2N) radiated power for different tracks (ISVR results at 160 km/h using TSI roughness as total roughness)

4.1 DEFINITION OF REFERENCE TRACKS

This section aims at defining reference tracks that can be used for the assessment of a rolling stock when no particular test track has to be modelled. The three different tracks that have been used for the benchmark are the following:

- Track 1: Monobloc sleeper ballasted track with 800 MN/m rail pads
- Track 2: Bi-bloc ballasted track with 350 MN/m rail pads
- Track 3: Slab-track with very soft rail mounting system

The rail sound power example of Figure 4-1 in fact refers to these three tracks. Due to its stiff rail pads, resulting in a high track decay rate, rail 1 radiates the lowest sound power. Track 3 in contrast leads to the highest rail sound power. Figure 4-3 shows the total radiated powers for the three tracks (with VB2N wheel). Indeed, track 3 radiates the highest sound power in the mid frequency range. In the presented example, the slab radiation is completely neglected. Due to the absence of sleepers, however, the low frequency radiation of slab tracks generally remains below the one of a ballasted track.

Note that a correct prediction of the slab track behaviour seems more difficult than for the ballasted tracks. Tracks 1 and 2 are therefore recommended for use as reference tracks. More detailed track parameters can be found in section 5 and appendix A.2. Calculation results for these tracks are also given in section 5.

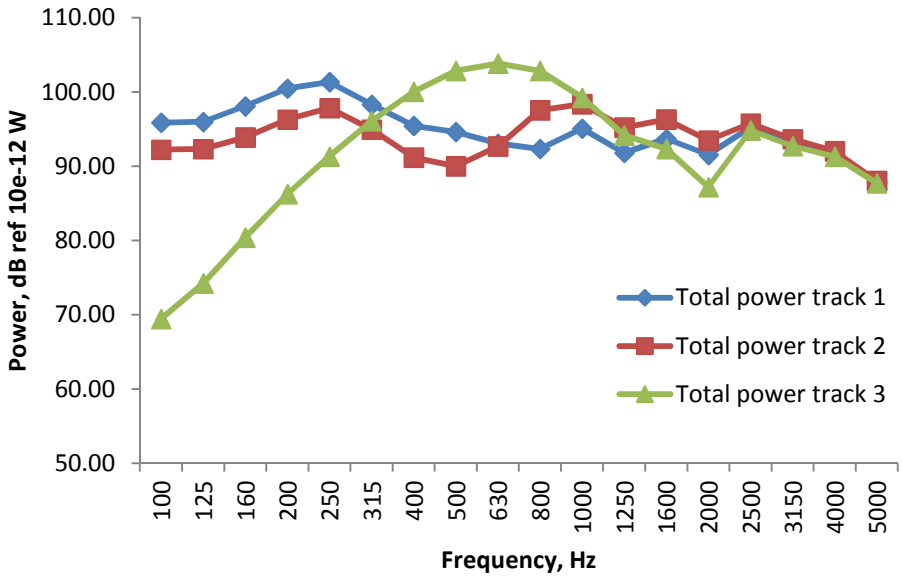

Figure 4-3 : Total radiated power (track + wheel) for different tracks, calculated decay rates (ISVR calculations at 160 km/h using TSI roughness as total roughness))

4.2 MODELLING HYPOTHESES

Rail model

As mentioned above, the track can be modelled fully analytically if certain simplifications are introduced. These simplifications notably include neglecting any cross-sectional deformation of the rail. Although models including these effects exist, their use is not necessary when focussing on the rolling stock. Modelling the rail as a continuously supported beam ("Timoshenko beam", RODEL model in TWINS) seems sufficient for this purpose.

Track decay rates

The properties of the rail, the rail pads, the sleepers and the ballast can be used in order to compute a track decay rate. However, TWINS tends to underestimate this decay rate; therefore a loss factor is often applied to the rail which is in reality not due to the steel itself but rather due to the interaction with the rail fastening system and the sleepers. In any case, the coherence between results obtained by different users can be improved by the use of measured track decay rates. In addition, measured track decay rates include the effect of the periodically supported rail and therefore improve the reliability of the computations when the rail model does neglect this effect. Their use is therefore recommended whenever adequate measurements are available. Alternatively, the TSI limit curves for track decay rates can be used in order to standardize calculations.

Vertical-lateral coupling

In a rail model such as RODEL, the rail is modelled as a beam without any coupling between vertical and lateral displacement. In reality, however, two different effects can lead to lateral excitation of the rail:

1. An off-central (vertical) excitation of the rail, and

2. The asymmetry introduced by the sleeper.

Effect 1 depends on the position of the contact point on the rail. For an unworn rail and wheel, the contact remains close to the centre, leading to a low lateral excitation. A cross coupling coefficient of – 12 dB is therefore recommended as a standard value. In special cases the coupling can be higher, which can be simulated using a cross coupling coefficient as low as - 7 dB.

Effect 2 only depends on the sleeper type: Each bloc of a bi-bloc sleeper is relatively symmetrical in respect to the rail, whereas a monobloc sleeper (modelled by taking into account its modal behaviour) introduces higher asymmetry. However, this effect is not believed to be dominating. Indeed, the lateral rail contribution can be high at frequencies with low lateral track decay rates, which are typically found around 1 to 2 kHz (see **Error! Reference source not found.**). Generally, the rail is already decoupled from the sleepers at these frequencies; therefore its behaviour does not depend on the sleeper type. Of course, the decoupling frequency between sleepers and rail depends on the rail pad stiffness, and the lateral track decay rate may already be low at frequencies below 1 kHz. Additional investigation is necessary in order to fully quantify the different effects.

Sleeper model

The use of a modal sleeper is recommended for monobloc sleepers.

Bi-bloc sleepers may be modelled as rigid masses. (N.B.: In TWINS, choosing between monobloc and bi-bloc sleepers actually means choosing between modal and mass sleeper model.)

Slab tracks can be modelled in different ways, taking into account or not the radiation of the slab. TWINS version 3.0 contains a slab track option that permits to introduce the dynamic behaviour of a concrete slab as well as its radiation. The rail can either be fixed directly on the slab (via a rail pad) or on sleepers lying on the slab. In the latter case, a second resilient layer can be introduced between sleeper and slab (defined through the “ballast” properties). The concerned sleeper must not necessarily be a real sleeper but can be a relatively small load distribution plate between the two pads. If the slab track option is not available, the slab track can directly be modelled as a bi-bloc sleeper track, which means neglecting the slab radiation. Two resilient layers can also be used here. In this case, a mass sleeper representing a load distribution plate is fixed between the lower rail pad (defined through the ballast properties) and the upper rail pad.

Ballast parameters

The ballast is generally not accounted for as a radiating surface, but its dynamic properties highly influence the behaviour of the track. TWINS provides a ballast stiffness file (blststif.to) based on measurements with monobloc sleepers that contains a frequency depending vertical stiffness and loss factor. For bi-bloc track (i.e. mass sleepers) the frequency dependent behaviour of the ballast has less importance, a constant value of 80 MN/m is often used. The lateral stiffness is set to a constant value in both cases (50 MN/m recommended). The loss factors of ballast are very high; when using a frequency independent loss factor, a value of 1 is recommended.

When working with slab tracks, a frequency dependent ground stiffness is needed in order to correctly model the behaviour of the concrete slab. For classical ballasted tracks, the influence of the ground is generally neglected (TWINS does not permit to enter a ground stiffness when using ballasted tracks).

4.3 TRACK MODELLING RECOMMENDATIONS OVERVIEW

The following tables recapitulate the recommended modelling assumptions and parameters for monobloc sleeper track, bi-block sleeper track and slab track.

Table 4-1: Track modelling recommendations overview (1)

		Monobloc (B70) sleeper track	Bi-bloc sleeper track	Slab track
Rail (indicated values are for UIC 60 rail)	Model	Beam on continuous support (Timoshenko / RODEL)		
	Vert.-lat. coupl	-12 dB[(1)]	-12 dB[(1)]	-12 dB[(1)]
	Vert.-lat. coupl sign	-1	-1	-1
	EI_V (Nm^2)	6.42E6	6.42E6	6.42E6
	EI_L (Nm^2)	1.06E6	1.06E6	1.06E6
	ρA (kg/m)	60	60	60
	κ (shear coff.)	0.4	0.4	0.4
	Loss fact. η_v[(5)]	0.02	0.02	0.02
	Loss fact. η_L[(5)]	0.02	0.02	0.02
Track decay rates		Measured track decay rates or TSI limit decay rates		Measured track decay rates
Rail pad	Stiff. Vert. (MN/m)	Depending on the considered track, for a TSI compliant track, values above 300 MN/m are coherent		Depending on the considered track
	Stiff. Lat. (MN/m)	If no distinct values are available, 10 to 20 % of the vertical stiffness can be assumed		
	Loss factor η_v	Depending on the considered track, generally 0.01 – 0.04		
	Loss factor η_L	Depending on the considered track, generally 0.01 – 0.04		
Sleeper	Model	Modal sleeper	Mass sleeper	Slab option[(3)]
	Mass (kg)	280	120	[(3)]
	Spacing (m)	0.6	0.6	0.6
	Width (m) [(2)]	0.3	0.29	Depends on "sleeper" type [(4)]
	Length (m) [(2)]	1.3	0.84	
	E-mod. (N/m^2)	4.13E+10	-	-

[(1)] For special cases (worn profiles, etc), a higher coupling around -7 dB can be used.
[(2)] These values relate to the radiation from the sleeper. Half a sleeper surface is therefore attributed to each rail.
[(3)] The "sleeper on slab" option permits to use a mass sleeper on the slab. It may be used for a concrete bi-bloc sleeper or a small steel load distribution plate.
[(4)] The load distribution plate of slab tracks may be completely shielded and therefore not taken into account as a radiating surface.
[(5)] This loss factor is needed for correct computation of decay rates (see discussion about track decay rates in section 4.2). Its value also depends on the rail pad stiffness; however, additional research is necessary in order to find better ways to compute correct decay rates.

Table 4-2 : Track modelling recommendations overview (2)

Ballast	Vertical stiffness (MN/m)	Function of frequency (blststif.to)[(1)]	80	Ballast properties can be used in TWINS to account for the “lower rail pad” (under sleeper pad)
	Lateral stiffness (MN/m)	50	50	
	Loss factor. η_v	Function of frequency (blststif.to) [(1)]	1.0	
	Loss factor. η_L	1.0	1.0	
Sound pressure level calculation	Receiver *x* position (m)	-1.2		
	Receiver *y* position (m)	6.75		
	Ground position for reflection below top of rail (m)	0.5		
	Flow resistivity (Rayls/m)	3E6[(2)]		
	Wheelsets	number of wheelsets per car		
	Wheels per axle	2 (taking into account of the opposite wheel)		
	Integration length (m)	car length		
	Accumulation length (m)	infinity (i.e. 0 in TWINS)		

[(1)] According to TWINS user’s manual recommendation (2)

[(2)] The flow resistivity only concerns the ground properties outside the track itself. Absorption of the ballast (in contrast to a concrete slab) is not directly taken into account.

5. EXAMPLE CALCULATIONS

In order to detect sources for discrepancies between calculations performed by different users, a set of benchmark cases had been defined that were treated by ISVR, TNO, D2S and VTC. ISVR, TNO and VTC used TWINS. D2S used a different model.

Some of the obtained results are reproduced here as example calculations. The discussion of the results obtained by different users is limited to the wheel sound powers, as the wheel part is especially critical for virtual homologation of rolling stock. For the remaining components, as well as total power and total SPL, the ISVR results are presented in order to give a complete set of example results.

The input data is recalled in section 5.1 (with further details in appendix A); results are summarized in section 5.2.

5.1 INPUT DATA DEFINITION

Wheels

Two different wheels have been used for the benchmark calculations; however, only computations using the VB2N wheel are presented in this report. The VB2N wheel is a straight 840 mm passenger coach wheel (see appendix A.1)

Tracks

The tracks that have been used for the benchmark calculations are defined in section 4.1. Only results for tracks 1 and 2 are discussed in this report, therefore no details about the slab track are given. Measured track decay rates (TDR) were available for track 2; these are given in Table 7-3 of appendix A.2.

The results produced by ISVR have been obtained by using the recommended values given in Table 4-1 and Table 4-2. The lateral rail pad stiffness has been assumed to 20 % of the vertical stiffness. The rail pad loss factors are $\eta_v = \eta_L = 20\%$. ISVR uses a cross coupling coefficient of -7 dB for track 1 (monobloc 800 MN/m) and – 12 dB for track 2 (bi-bloc 350 MN/m). See also the discussion concerning the vertical-lateral coupling in section 4.2.

Load

A static wheel load of 50 kN is assumed for all calculations.

Speed

A speed of 160 km/h is assumed for the presented calculations.

Roughness

TSI roughness as given in appendix A.3 is used. The contact filter according to Eq. 2-2 is applied.

5.2 DISCUSSION OF RESULTS

This section gives an outline of the obtained results; details can be found in appendix B. As mentioned above, the analysis of dispersion between results obtained by different users is limited to the wheel results. As the D2S model does directly deliver SPL due to each component, sound powers have not been communicated and are therefore not integrated here.

Wheel modal frequencies

The dispersion between the different calculations of natural frequencies is very low despite the use of different types of models (axis-symmetric and 3D). Details are found in appendix B.1.

Wheel sound power

Wheel sound powers calculated by the different users are in good agreement. Using the same contact filter model (Remington), the difference remains below 0.5 dB(A).

The good agreement of the different wheel calculations is an encouraging result for virtual homologation procedures.

Measured vs. calculated Track Decay Rates (TDR)

For track 2, measured TDR were available; these are compared to ISVR calculations in appendix B.3. The TDR for track 2 can reasonably be approached by calculations. The decrease of the TDR due to a decoupling of the rail on the stiffness of the rail pads is well reproduced. A certain discrepancy at higher frequencies may be due to deformations of the rail cross-section that is neglected in the present calculations.

As mentioned before, measured TDR should be used when available in order to additionally increase the coherence between results obtained by different users.

Rail sound power

Rail sound powers are presented in appendix B.4. The different behaviour of the two tracks (higher rail power for softer rail pads) as well as the influence of the TDR is clearly visible.

Sleeper sound power

Sleeper sound powers are presented in appendix B.5. As expected, the track with stiffer rail pads leads to a higher sleeper sound power.

Total sound power

Total sound power is given in appendix B.6. Due to a partial compensation between rail and sleeper powers, the total radiated powers are relatively close for the two different tracks.

Total sound pressure

Total sound pressure is given in appendix B.7. Again, the differences between the two tracks is small in respect to the average dB(A) value.

6. CONCLUSION

This report defines procedures for modelling wheels and tracks. Special attention is paid to parameters that are generally regarded as second order parameters and for which different “default” values are often used by different users. The benchmark calculations, performed by ISVR, TNO, D2S and VTC have helped to define these parameters. The examples given in the last section can serve as reference solutions.

7. REFERENCES

1. **Marcel H.A. Janssens, D.J. Thompson, F.G. de Beer.** *TWINS version 3.0, Track-Wheel Interaction Noise Software, Theoretical manual.* 1999.

2. —. *TWINS version 3.0, Track-Wheel Interaction Noise Software, User's manual.* 2000.

3. *EUROPEAN STANDARD EN 13979-1 : Railway applications. Wheelsets and bogies. Monobloc wheels . Technical approval procedure . Part 1: Forged and rolled wheels.*

4. **Remington, P.J.** Wheel/rail noise part IV: Rolling noise. *Journal of Sound and Vibration.* Vol. 46, 1975.

5. **Remington, P.J. and Webb, J.** Estimation of wheel/rail interaction forces in the contact area due to roughness. *Journal of Sound and Vibration.* Vol. 193, 1996.

6. **Thompson, D.J.** The influence of the contact zone on the excitation of wheel/rail noise. *Journal of Sound and Vibration.* Vol. 267, 2003.

7. —. *Railway Noise and Vibration.* s.l. : Elsevier, 2009.

8. *Commission Decision of 23 December 2005 concerning the technical specification for interoperability (« TSI ») relating to the subsystem 'rolling stock', Official Journal of the European Union, 18.2.2006.*

A. APPENDIX A: BENCHMARK INPUT DATA

A.1 : WHEELS

Geometrical data for the VB2N wheel is summarized in Table 7-1, as given by ISVR.

Figure 7-1 shows a drawing of the VB2N wheel. A CAD file of this wheel had been provided for the benchmark calculations.

Table 7-1 : Geometrical wheel data (ISVR) for VB2N wheel

Hub radius (m)	0.1542
Web position 1 (m)	0.176
Web position 2 (m)	0.2183
Web position 3 (m)	0.262
Web position 4 (m)	0.3057
Web position 5 (m)	0.3473
Inner tyre radius (m)	0.37
Wheel radius (m)	0.42
Tread width (m)	0.135
Web thickness (m)	0.021
Contact position from flange back (m)	0.07±0.01

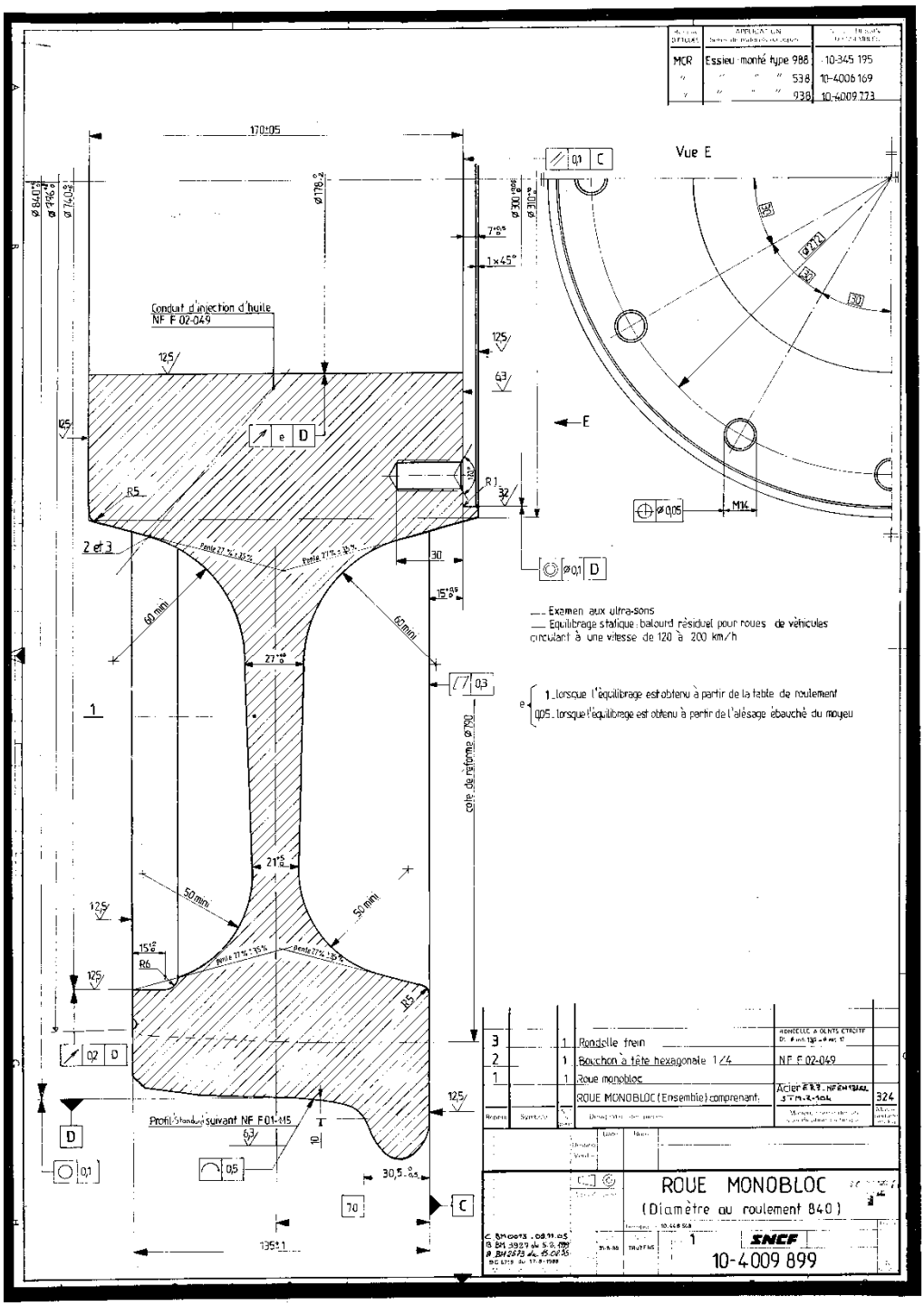

Figure 7-1 : VB2N wheel drawing

Rail of type UIC 60 with a new rail head of 0.3 m radius has been assumed for all tracks.

Ballasted track parameters

The ballasted tracks rail pads parameters have only been defined in vertical direction: 800 MN/m dynamic stiffness for track 1 and 350 MN/m dynamic stiffness for track 2. Sleeper parameters are given in the following table.

Table 7-2 : Sleeper parameters (U70 monobloc and bi-bloc)

	Track 1: MONOBLOC	Track 2: BI-BLOC	
Sleeper mass	280/2	120	kg
Sleeper spacing	0.6	0.6	m
Sleeper Length (L)	2.6	0.84	m
Sleeper Width (top) (bottom at end) (bottom at centre)	0.15 0.30 0.24	0.21 0.29 N/A	m
Sleeper Height (at end) (at centre)	0.21 0.175	0.24 N/A	m
Parameters for modal sleeper model:			
Sleeper Young's modulus	0.413E11	N/A	Pa
Sleeper Poisson's ratio	0.15	N/A	
Sleeper Density	2750	N/A	kg/m^3
Sleeper Loss factor	0.02	N/A	

Track decay rates

Calculated as well as measured track decay rates (TDR) have been used for the benchmark calculations, given in the following table:

Table 7-3 : Measured track decay rates

	Track decay rates for **Track 2,** measured on french HS bi-bloc track (SNCF)	
fc	TDRvert	TDRlat
100	9.8	8.9
125	9.5	7.5
160	13.3	5.8
200	13.6	4.1
250	12.5	3.7
315	14.7	2.9
400	16.0	1.3
500	13.3	0.7
630	7.3	0.9
800	3.0	0.8
1000	1.3	0.4
1250	4.8	0.3
1600	1.9	1.0
2000	1.0	1.2
2500	0.9	2.5
3150	1.7	6.1
4000	3.3	2.6
5000	14.1	0.8

A.3 : ROUGHNESS

The TSI+ limit curve (8) for rail roughness has been used as a combined wheel-rail roughness.

Table 7-4: TSI+ roughness

Wavelength (cm)	*Roughness dB(ref 1 µm)*
63.4	21.1
50.4	19.1
40.0	17.1
31.8	15.0
25.2	13.0
20.0	11.0
15.9	9.0
12.6	7.0
10.0	4.9
8.0	2.9
6.3	0.9
5.0	-1.1
4.0	-3.2
3.2	-5.0
2.5	-5.6
2.0	-6.2
1.6	-6.8
1.3	-7.4
1.0	-8.0
0.8	-8.6
0.6	-9.2
0.5	-9.8
0.4	-10.4
0.3	-11.0

B. APPENDIX B : BENCHMARK CALCULATIONS

B.1 : WHEEL MODELLING AND WHEEL MODES

VB2N wheel

The VB2N wheel has been provided as a CAD file. Meshing is performed by the users. ISVR and VTC used an axis-symmetrical model; TNO used a 3D model (see Figure 7-2).

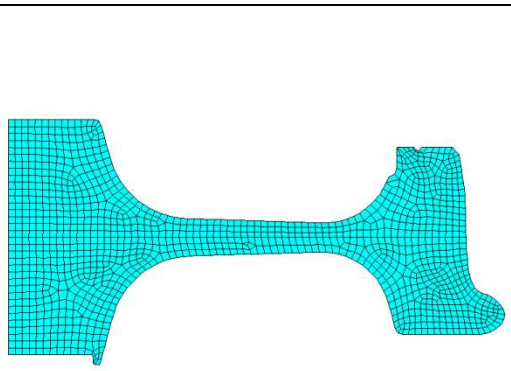

Axis-symmetrical mesh by ISVR

3D mesh by TNO

Figure 7-2: Meshing of VB2N wheel performed by ISVR and TNO

Table 7-5: Natural frequencies of VB2N wheel modes

Mode	Natural freq. [Hz] ISVR	Natural freq. [Hz] TNO	Natural freq. [Hz] VTC
R,2	2287.1	2249	2304.5
R,3	2876.8	2828	2898.8
R,4	3550.8	3490	3577.9
1L,2	2680.7	2642	2701.3
1L,3	3333.5	3287	3359.1
1L,4	4066.9	4014	4098.2

For natural frequencies of the VB2N wheel, the maximum dispersion is of approximately 2.5 %. The differences between results obtained with a 3D model and a 2D model are slightly higher than the differences between both 2D models.

B.2 : WHEEL SOUND POWER RESULTS

Overall dB(A) values are compared in Table 7-6. Spectra are given in Figure 7-3 and Figure 7-4. Note that the wheel radiated power is essentially due to frequencies above 2 kHz for this wheel. Results show a very small dispersion in this frequency band. The slightly higher sound powers found by TNO are mainly due to the use of the DPRS contact filter model. As expected, wheel sound power is also very similar for both tracks. The differences at low frequencies are caused by slightly different track behaviour and do not influence the overall power in dB(A). Note that the presented spectra are not A-weighted.

Table 7-6 : Wheel sound power results in dB(A)

	ISVR	TNO	VTC
VB2N on track 1	100.1	101.3	100.9
VB2N on track 2	99.9	101.3	100.3

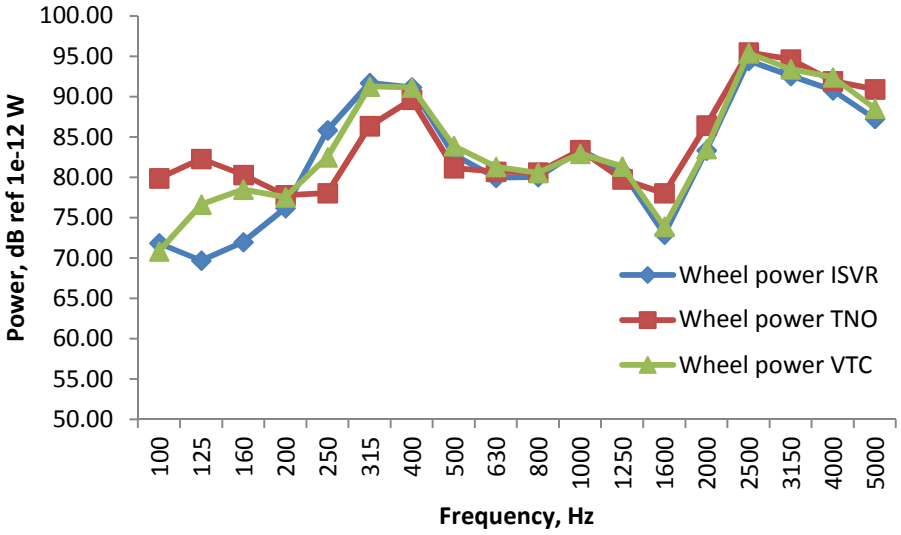

Figure 7-3 : Wheel sound power case 1 (VB2N on track 1 at 160 km/h)

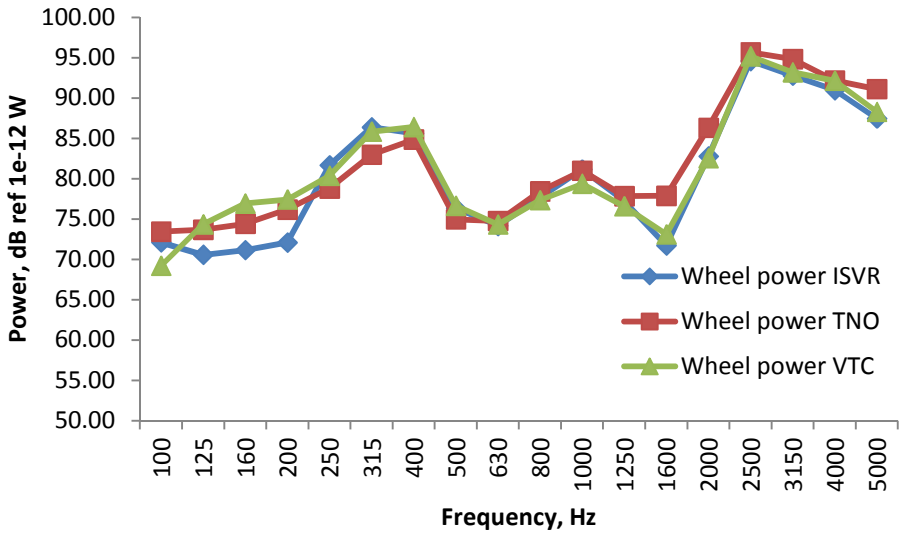

Figure 7-4: Wheel sound power case 2 (VB2N on track 2 at 160 km/h)

B.3 : TRACK DECAY RATES

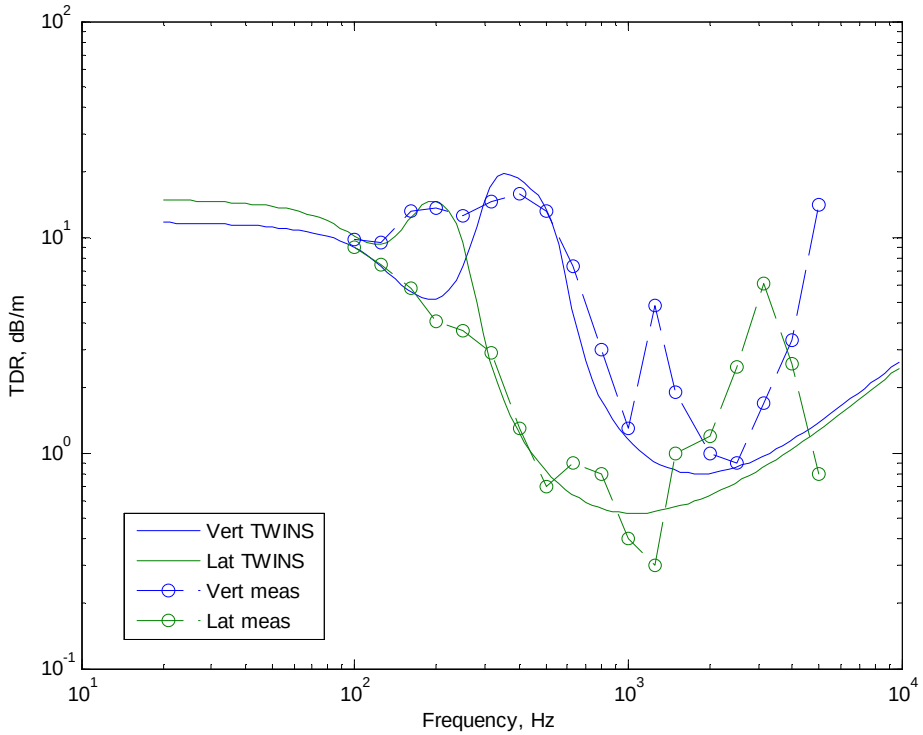

Figure 7-5: Comparison of measured and calculated decay rates, bi-bloc track, ISVR

B.4 : RAIL SOUND POWER RESULTS

The rail sound powers in dB(A) for the different track are compared in Table 7-7. As expected, the track with softer rail pads leads to a higher rail sound power. Also note that the use of calculated TDR leads to a significantly higher rail power here, which is caused by the under-estimation of the TDR above 1 kHz.

Table 7-7: Rail sound power results in dB(A)

Case 1 (VB2N on Track 1), **Calculated TDR**	101.1
Case 2 a (VB2N on Track 2), **Calculated TDR**	104.3
Case 2 b (VB2N on Track 2), **Measured TDR**	102.1

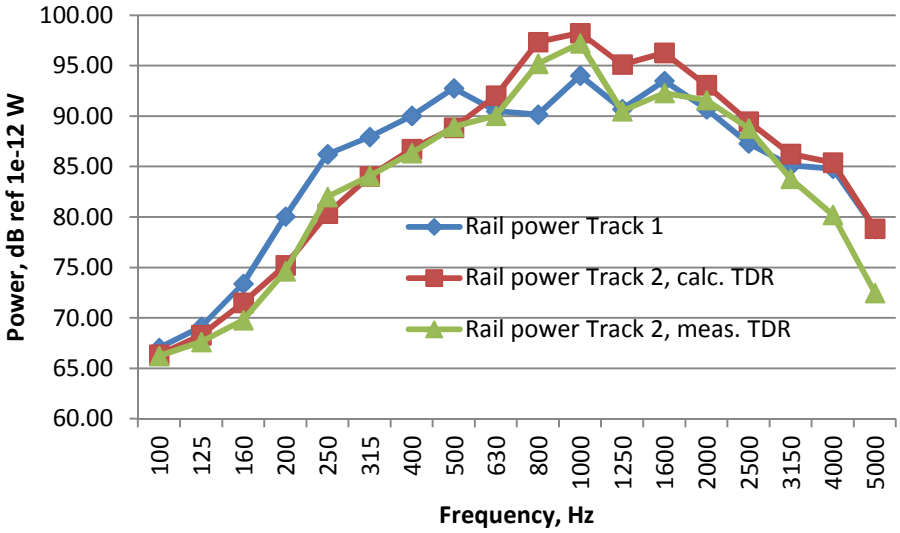

Figure 7-6 : Rail sound power for Tracks 1 and 2 (ISVR calculations)

B.5 : SLEEPER SOUND POWER RESULTS

Calculated sleeper powers are compared in Table 7-8; spectra are given in Figure 7-7. As expected, the stiffer rail pads of track 1 lead to a higher sleeper noise radiation. Some difference is also observed between computations with calculated and measured TDR, mainly caused by the gap around 200 Hz (see Figure 7-5).

Table 7-8: Sleeper sound power results in dB(A)

Case 1 (VB2N on Track 1), **Calculated TDR**	98.3
Case 2 a (VB2N on Track 2), **Calculated TDR**	94.0
Case 2 b (VB2N on Track 2), **Measured TDR**	92.8

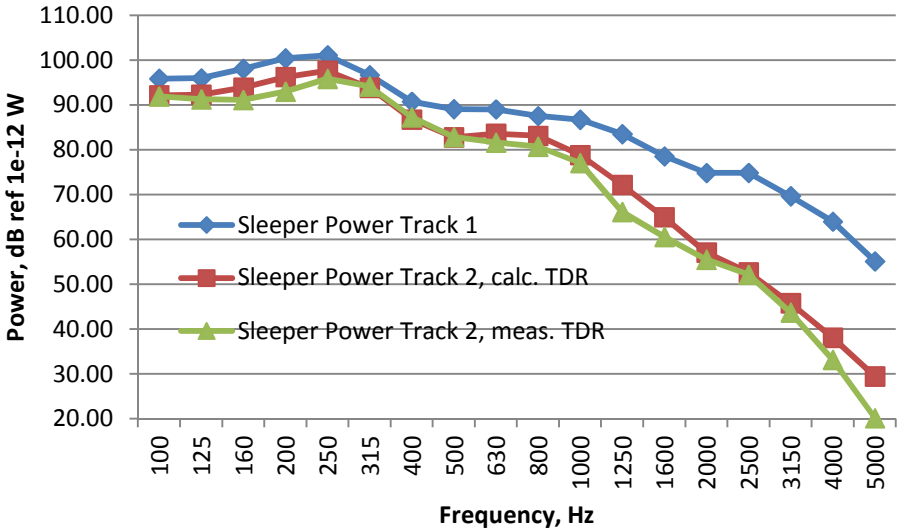

Figure 7-7 : Sleeper sound power for Tracks 1 and 2 (ISVR calculations)

B.6 : TOTAL SOUND POWER RESULTS

Calculated total powers are compared in Table 7-9, spectra are given in Figure 7-8. As track 1 is noisier in the low frequency range, and track 2 is noisier in the mid-frequency range, the difference is relatively small.

Table 7-9: Total sound power results in dB(A)

Case 1 (VB2N on Track 1), **Calculated TDR**	104.7
Case 2 a (VB2N on Track 2), **Calculated TDR**	105.9
Case 2 b (VB2N on Track 2), **Measured TDR**	104.4

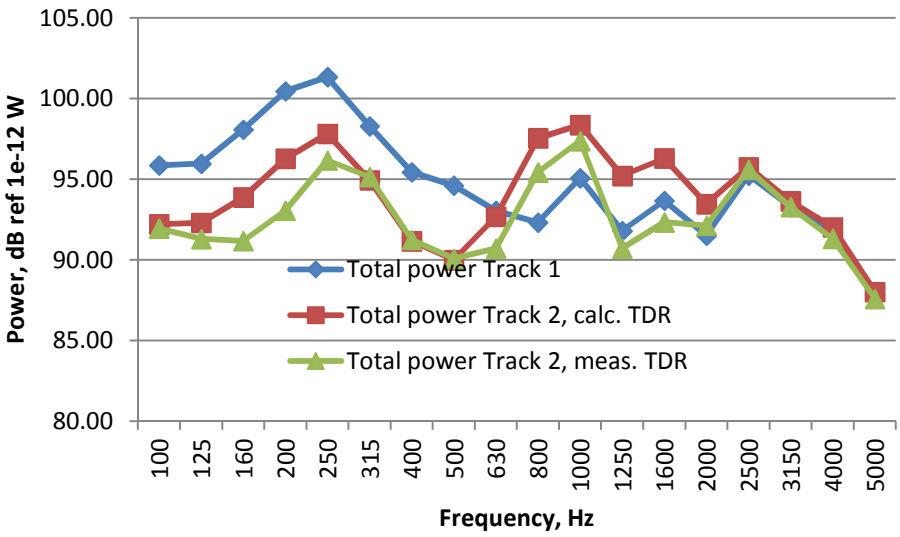

Figure 7-8 : Total sound power for Tracks 1 and 2 (ISVR calculations)

B.7 : TOTAL SOUND PRESSURE RESULTS

Calculated total sound pressure is given in Table 7-10 and Figure 7-9. Note that taking into account of the (frequency dependent) ground reflection introduces an additional filtering.

Table 7-10: Total sound pressure results in dB(A)

Case 1 (VB2N on Track 1), **Calculated TDR**	86.6
Case 2 a (VB2N on Track 2), **Calculated TDR**	86.2
Case 2 b (VB2N on Track 2), **Measured TDR**	85.0

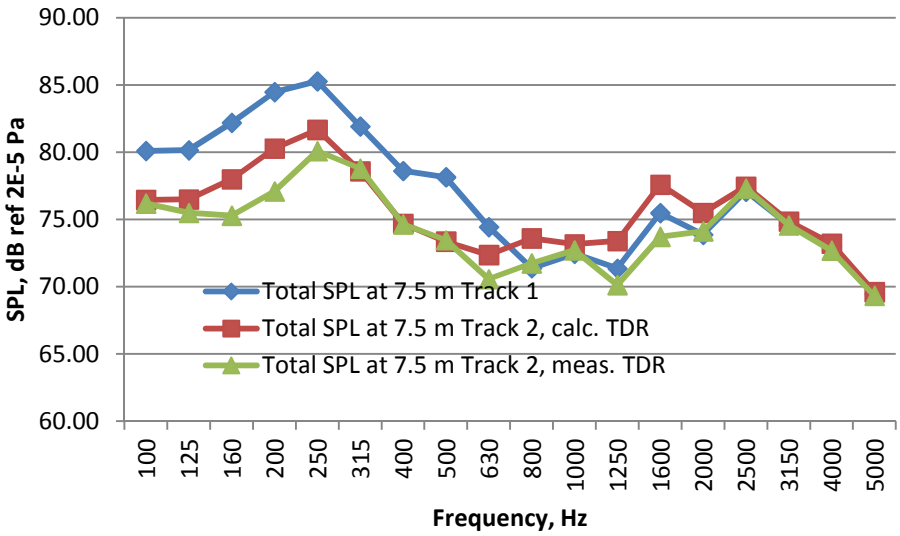

Figure 7-9 : Total sound pressure for Tracks 1 and 2 (ISVR calculations)